Hz. The spectrum is therefore consistent with the solid-state structure. The ^1H NMR spectra of **6** to **11** recorded immediately after dissolution are equally well seen to be consistent with the presence of the two dithiophosphate groups and hence consistent with the solid-state structure of **7**. However, while the ^1H NMR spectra of **1–5** show no change when re-recorded after some time, the spectra of **6–11**, each show the appearance of an additional set of peaks of the same multiplicity and relative heights of the original set. Thus, **6–11** undergo isomerism in solution while **1–5** do not.

Acknowledgment. We thank the Natural Sciences and Research Council of Canada for financial support.

Registry No. **1**, 106799-90-0; **2**, 106799-91-1; **3**, 106799-92-2; **4**, 106799-93-3; **5**, 106799-94-4; **6**, 106820-90-0; **7**, 106820-91-1; **8**, 106820-92-2; **9**, 106820-93-3; **10**, 106820-94-4; **11**, 106820-95-5; *O,O'*-dimethyl dithiophosphate, 756-80-9; (*p*-methoxyphenyl)-tellurium tribromide, 36309-69-0; diphenyltellurium dichloride, 1206-36-6.

Supplementary Material Available: Unit cell packing diagrams, tables of anisotropic thermal parameters for non-hydrogen atoms, and tables of final fractional coordinates and thermal parameters for hydrogen atoms (7 pages); tables of observed and calculated structure factors (30 pages). Ordering information is given on any current masthead page.

Structural and Bonding Features of the Methoxymethylidyne Ligand in Cluster Complexes. X-ray Crystal Structures of $Co_3(\mu_3\text{-}COCH_3)(CO)_9$ and $Fe_3(\mu_3\text{-}COCH_3)(\mu\text{-}CO)_2(CO)_6(\eta\text{-}C_5H_5)$

Alison A. Aitchison and Louis J. Farrugia*

Department of Chemistry, University of Glasgow, Glasgow G12 8QQ, Scotland, U.K.

Received September 22, 1986

The methoxymethylidyne cluster complexes $Co_3(\mu_3\text{-}COCH_3)(CO)_9$ (**1**) and $Fe_3(\mu_3\text{-}COCH_3)(\mu\text{-}CO)_2(CO)_6(\eta\text{-}C_5H_5)$ (**2**) have been examined by X-ray diffraction. Complex **1** crystallizes in the triclinic space group $P\bar{1}$ (No. 2) with a = 8.0125 (6) Å, b = 8.3823 (4) Å, c = 12.3052 (7) Å, α = 93.011 (5)°, β = 102.025 (5), γ = 104.890 (5)°, V = 777.12 (9) Å^3, and D_{calcd} = 2.02 g cm^{-3} for Z = 2 and M_r 471.94. Data were collected for $1.5 \leq \theta \leq 30°$ with graphite-monochromated X-radiation (Mo Kα). The structure was refined to R = 0.026 (R_w = 0.035) for 3528 observed reflections [$I \geq 2.5\sigma(I)$]. The three Co–Co separations are identical within error [Co(1)–Co(2) = 2.478 (1), Co(1)–Co(3) = 2.478 (1), and Co(2)–Co(3) = 2.480 (1) Å], while there is a slight but significant asymmetry in the $Co_3(\mu_3\text{-}C)$ moiety [Co(1)–C(10) = 1.882 (2), Co(2)–C(10) = 1.912 (2), and Co(3)–C(10) = 1.906 (2) Å]. The plane of the $\mu_3\text{-}COCH_3$ ligand is perpendicular to the Co(2)–Co(3) vector (angle between normal to plane and Co–Co = 0.63°), resulting in near idealized mirror symmetry for **1**. Complex **2** crystallizes in the monoclinic space group $P2_1/n$ (No. 14) with a = 9.336 (2) Å, b = 18.896 (2) Å, c = 9.936 (2) Å, β = 99.65 (2)°, V = 1728.0 (6) Å^3, and D_{calcd} = 1.92 g cm^{-3} for Z = 4 and M_r 499.7. Data were collected as above for $2 \leq \theta \leq 25°$ with the structure refined to R = 0.032 (R_w = 0.044) for 2131 observed [$I \geq 2.5\sigma(I)$] data. The triiron triangle [Fe(1)–Fe(2) = 2.582 (1), Fe(1)–Fe(3) = 2.547 (1), and Fe(2)–Fe(3) = 2.524 (1) Å] is capped by a slightly asymmetric $\mu_3\text{-}COCH_3$ ligand [Fe(1)–C(9) = 1.905 (5), Fe(2)–C(9) = 1.935 (5), and Fe(3)–C(9) = 1.952 (5) Å]. The two μ-carbonyl ligands bridge to the unique iron atom, which also bears the cyclopentadienyl group, while both the other iron atoms are ligated to three terminal carbonyl groups. Although the cluster fragment "$Fe_3(\mu\text{-}CO)_2(CO)_6(\eta\text{-}C_5H_5)$" has pseudomirror symmetry, the orientation of the $\mu_3\text{-}COCH_3$ ligand, approximately parallel to the Fe(1)–Fe(2) axis (angle between normal to plane and Fe–Fe = 90.39°) removes this symmetry element from **2**. Extended Hückel MO calculations on **1** and **2** show that the differing observed orientations of the $COCH_3$ group lie close in energy, with a small barrier to rotation or inversion. The bonding capabilities of the $COCH_3$ moiety have similarities to both CO and the alkylidyne ligand CR. Calculations on the model complexes $Fe_3(\mu\text{-}H)(\mu\text{-}CR)(CO)_{10}$ (R = H, OCH_3) allow a rationalization of the differing "semi-μ_3" interactions found in related osmium species and indicate that their divergent electrophilic behavior may be frontier orbital controlled.

Introduction

Since the initial report by Shriver et al.[1] on the methylation of the bridging carbonyl ligand in $[Fe_3(\mu\text{-}H)(\mu\text{-}CO)(CO)_{10}]^-$ resulting in the methoxymethylidyne complex $Fe_3(\mu\text{-}H)(\mu\text{-}CR)(CO)_{10}$ (**1a**, R = OCH_3), several other cluster species including the ruthenium[2] and osmium[3] analogues of **1a** have been prepared by similar routes. Polynuclear compounds containing the $COCH_3$ ligand bridging two, three, and four metal atoms are now known. Examples in the first class include $[Fe_2(\mu\text{-}COCH_3)(\mu\text{-}CO)(Ph_2PCH_2CH_2PPh_2)(\eta\text{-}C_5H_5)_2]^+$ (providing a rare example of synthesis by alkylation of a *neutral* carbonyl complex)[4] and the recently reported[5] $FeMn(\mu\text{-}COCH_3)(\mu$-

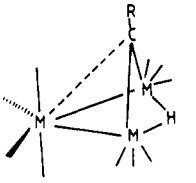

$M_3(\mu\text{-}H)(\mu\text{-}CR)(CO)_{10}$

(M = Fe; R = OCH_3 **1a**, R = H **1b**)
(M = Os; R = H **2a**, R = OCH_3 **2b**,
R = Ph **2c**, R = CH_2CHMe_2 **2d**)

(1) Shriver, D. F.; Lehman, D.; Strope, D. *J. Am. Chem. Soc.* **1975**, *97*, 1594.
(2) Johnson, B. F. G.; Lewis, J.; Orpen, A. G.; Raithby, P. R.; Süss, G. *J. Organomet. Chem.* **1979**, *173*, 187.
(3) Gavens, P. D.; Mays, M. J. *J. Organomet. Chem.* **1978**, *162*, 389.

0276-7333/87/2306-0819$01.50/0

$CO)(CO)_2(\eta\text{-}C_5H_5)(\eta\text{-}C_5H_4Me)$. An interesting example of the latter class is the complex $Fe_4(\mu\text{-}H)(\mu_4\text{-}\eta^2\text{-}COCH_3)(CO)_{12}$ that contains[6] a unique $\mu_4\text{-}\eta^2\text{-}COCH_3$ group where the C–O coordination to the metal framework is similar to that of the $\mu_4\text{-}\eta^2$-CO ligand in the precursor anion $[Fe_4(\mu\text{-}H)(\mu_4\text{-}\eta^2\text{-}CO)(CO)_{12}]^-$.[7] Several heteronuclear methoxymethylidyne species have been reported,[5,8-13] although only one example has been synthesized by O-alkylation of a heteronuclear carbonyl complex.[5]

The methoxymethylidyne ligand has variously been described as an O-alkylated carbonyl group,[1,3,14] or a μ-carbyne[2] with the alkoxyalkylidyne formalism favored[15] in view of the downfield chemical shift of the bridging carbon nucleus observed in these systems. The partial multiple-bond character of the C–O bond has been ascribed to π donation from the heteroatom,[2,16] and this implied charge transfer has been held responsible for the lesser electrophilic character of the alkylidyne complexes.[17] The unsubstituted μ-methylidyne ligand in $Os_3(\mu\text{-}H)(\mu_3\text{-}CR)(CO)_{10}$ (**2a**, R = H) has been shown to be highly susceptible to nucleophilic attack,[17] and remarkably in the cationic dinuclear species $[Fe_2(\mu\text{-}CH)(\mu\text{-}CO)(CO)_2(\eta\text{-}C_5H_5)_2]^+$ the μ-CH ligand is electrophilic enough to form an adduct with CO.[18] By contrast the $\mu\text{-}COCH_3$ ligand is much less reactive,[14] and although complex **2a** arises[17] from a *formal* nucleophilic attack at the alkylidyne carbon atom of $Os_3(\mu\text{-}H)(\mu\text{-}CR)(CO)_{10}$ (**2b**, R = OCH_3), recent results[19] show that the mechanistic pathway to the phenyl analogue[20] **2c**, R = Ph, is more complex.

Dinuclear compounds containing μ-CR ligands with alkyl or aryl substituents are reactive toward transition-metal-centered nucleophiles, and this route has been successfully exploited for the designed synthesis of a number of cluster complexes containing μ_3-alkylidyne groups[21]. Reactivity is centered on the alkylidyne carbon,

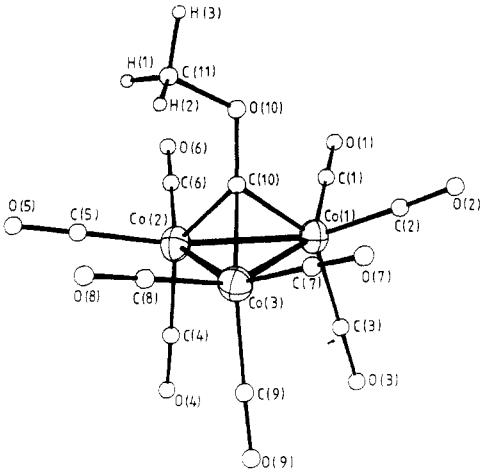

Figure 1. Molecular geometry and atomic labeling scheme for the complex $Co_3(\mu_3\text{-}COCH_3)(CO)_9$ (**3a**).

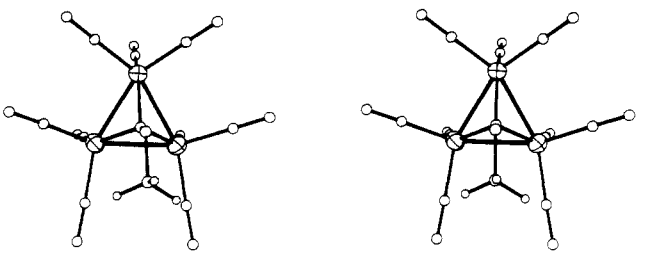

Figure 2. Stereoview of $Co_3(\mu_3\text{-}COCH_3)(CO)_9$ showing orientation of $COCH_3$ group.

and in most cases a new bond between this atom and the incoming transition metal is formed. However, alkoxyalkylidyne complexes do not appear to show similar reactivity. Although complex **1a** reacts with $Pt(C_2H_4)_2(PPh_3)$ to give $Fe_3Pt(\mu_3\text{-}H)(\mu_3\text{-}COCH_3)(CO)_{10}(PPh_3)$,[8] the $\mu_3\text{-}COCH_3$ ligand is not bonded to the platinum atom. By way of contrast the osmium analogue **2b** on treatment with $Pt(C_2H_4)_2(PCy_3)$ (Cy = c-C_6H_{11}) affords[22] the unusual pentanuclear complex $Os_3Pt_2(\mu\text{-}H)(\mu\text{-}OCH_3)(\mu_5\text{-}C)(CO)_9(PCy_3)_2$ resulting from cleavage of the C–O bond of the methoxymethylidyne ligand. Furthermore **1a** affords the species $Fe_2Me(\mu\text{-}H)(\mu_3\text{-}COCH_3)(CO)_7(\eta\text{-}C_5H_5)$ (M = Co,[11] M = Rh[12]) on treatment with $M(CO)_2(\eta\text{-}C_5H_5)$ in a reaction whereby the $Fe(CO)_4$ moiety in **1a** is replaced by the isolobal[23] fragment $M(CO)(\eta\text{-}C_5H_5)$. These results show that the reduced electrophilicity in alkoxymethylidyne complexes leads to diverse reaction pathways not involving attack at the alkylidyne carbon center.

In this context we herein report X-ray studies on $Co_3(\mu_3\text{-}COCH_3)(CO)_9$ and $Fe(\mu_3\text{-}COCH_3)(\mu\text{-}CO)_2(CO)_6(\eta\text{-}C_5H_5)$ and semiquantitative EHMO calculations on these and related molecules in order to enhance our understanding of the structure, bonding, and reactivity of the $COCH_3$ ligand, and we also discuss the incipient "semi-μ_3" interaction found in these systems.

Results and Discussion

Treatment of $Fe_3(\mu\text{-}H)(\mu\text{-}COCH_3)(CO)_{10}$ (**1a**) with $Co_2(CO)_8$ at 90 °C for 12 h gave reasonable yields of the tricobalt alkylidyne complex $Co_3(\mu_3\text{-}CR)(CO)_9$ (**3a**, R = OCH_3). **3a** was characterized by ^1H NMR, IR, and high-resolution mass spectroscopies. The spectral results obtained for **3a** agree with previously reported[24] data for the

(4) La Croce, S. J.; Menard, K. P.; Cutler, A. R. *J. Organomet. Chem.* **1980**, *190*, C79.
(5) Fong, R. H.; Hersh, W. H. *Organometallics* **1985**, *4*, 1468.
(6) (a) Whitmire, K.; Shriver, D. F.; Holt, E. M. *J. Chem. Soc., Chem. Commun.* **1980**, 780. (b) Dawson, P. A.; Johnson, B. F. G.; Lewis, J.; Raithby, P. R. *J. Chem. Soc., Chem. Commun.* **1980**, 781.
(7) Manassero, M.; Sansoni, M.; Longoni, G. *J. Chem. Soc., Chem. Commun.* **1976**, 919.
(8) Green, M.; Mead, K. A.; Mills, R. M.; Salter, I. D.; Stone, F. G. A.; Woodward, P. *J. Chem. Soc., Chem. Commun.* **1982**, 51.
(9) Farrugia, L. J.; Freeman, M. J.; Green, M.; Orpen, A. G.; Stone, F. G. A.; Salter, I. D. *J. Organomet. Chem.* **1983**, *249*, 273.
(10) Bateman, L. W.; Green, M.; Mead, K. A.; Mills, R. A.; Salter, I. D.; Stone, F. G. A.; Woodward, P. *J. Chem. Soc., Dalton Trans.* **1983**, 2599.
(11) Aitchison, A. A.; Farrugia, L. J. *Organometallics* **1986**, *5*, 1103.
(12) Farrugia, L. J. *J. Organomet. Chem.* **1986**, *310*, 67.
(13) Farrugia, L. J. *Acta Crystallogr., Sect. C: Cryst. Struct. Commun.* **1986**, *C42*, 680.
(14) Hodali, H. A.; Shriver, D. F. *Inorg. Chem.* **1979**, *18*, 1236.
(15) Keister, J. B.; Payne, M. W.; Muscatella, M. J. *Organometallics* **1983**, *2*, 219.
(16) Xiang, S. F.; Bakke, A. A.; Chen, H.-W.; Eyermann, C. J.; Hoskins, J. L.; Lee, T. H.; Seyferth, D.; Withers, H. P., Jr.; Jolly, W. L. *Organometallics* **1982**, *1*, 699.
(17) Shapley, J. R.; Cree-Uchiyama, M. E.; St. George, G. M. *J. Am. Chem. Soc.* **1983**, *105*, 140.
(18) Casey, C. P.; Fagan, P. J.; Day, V. W. *J. Am. Chem. Soc.* **1982**, *104*, 7360.
(19) Shapley, J. R.; Yeh, W.-Y.; Churchill, M. R.; Li, Y.-J. *Organometallics* **1985**, *4*, 1898.
(20) Yeh, W.-Y.; Shapley, J. R.; Li, Y.-J.; Churchill, M. R. *Organometallics* **1985**, *4*, 767.
(21) (a) Stone, F. G. A. *Pure Appl. Chem.* **1986**, *58*, 529. (b) Stone, F. G. A. *Angew. Chem., Int. Ed. Engl.* **1984**, *23*, 89. (c) Stone, F. G. A. In *Inorganic Chemistry Towards the 21st Century*; Chisholm, M. H., Ed.; ACS Symposium Series 211; American Chemical Society: Washington, DC, 1983; pp 383–397.
(22) Farrugia, L. J.; Miles, A. D.; Stone, F. G. A. *J. Chem. Soc., Dalton Trans.* **1985**, 2437.
(23) Hoffmann, R. *Angew. Chem., Int. Ed. Engl.* **1982**, *21*, 711.

Table I. Atomic Positional (Fractional Coordinate) Parameters with Estimated Standard Deviations in Parentheses for the Complex $Co_3(\mu_3\text{-}COCH_3)(CO)_9$ (3a)

	x/a	y/b	z/c
Co(1)	−0.22004 (4)	0.21409 (3)	−0.12201 (2)
Co(2)	−0.09105 (4)	0.15498 (3)	−0.28086 (2)
Co(3)	−0.34071 (4)	0.28345 (3)	−0.31030 (2)
O(1)	0.0770 (3)	0.2012 (3)	0.0572 (2)
O(2)	−0.3410 (3)	0.4448 (3)	0.0075 (2)
O(3)	−0.4826 (3)	−0.1084 (3)	−0.1241 (2)
O(4)	−0.2964 (4)	−0.1952 (3)	−0.3485 (2)
O(5)	0.0315 (4)	0.2298 (3)	−0.4836 (2)
O(6)	0.2484 (3)	0.1376 (4)	−0.1483 (2)
O(7)	−0.5126 (4)	0.5215 (3)	−0.2359 (2)
O(8)	−0.3006 (3)	0.4167 (3)	−0.5200 (2)
O(9)	−0.6415 (3)	−0.0161 (3)	−0.3845 (2)
O(10)	0.0025 (2)	0.5074 (2)	−0.1823 (1)
C(1)	−0.0380 (3)	0.2052 (3)	−0.0128 (2)
C(2)	−0.2972 (3)	0.3548 (3)	−0.0424 (2)
C(3)	−0.3815 (3)	0.0146 (3)	−0.1228 (2)
C(4)	−0.2182 (4)	−0.0616 (3)	−0.3212 (2)
C(5)	−0.0170 (4)	0.2037 (3)	−0.4052 (2)
C(6)	0.1161 (4)	0.1438 (4)	−0.1991 (2)
C(7)	−0.4453 (4)	0.4303 (3)	−0.2643 (2)
C(8)	−0.3148 (4)	0.3645 (3)	−0.4390 (2)
C(9)	−0.5264 (4)	0.0976 (3)	−0.3569 (2)
C(10)	−0.1100 (3)	0.3588 (2)	−0.2140 (2)
C(11)	0.0704 (4)	0.5990 (3)	−0.2648 (3)
H(1)	0.137 (5)	0.541 (4)	−0.293 (3)
H(2)	0.155 (4)	0.718 (4)	−0.225 (2)
H(3)	−0.028 (5)	0.616 (5)	−0.320 (3)

complex. The complete transfer of the alkylidyne moiety from one set of metal centers to another is a somewhat unusual though not unprecedented event,[25,26] and a similar transfer reaction between the mononuclear alkylidyne complex $Cr(\equiv CCH_3)(CO)_4Br$ and $Co_2(CO)_8$ to give $Co_3(\mu_3\text{-}CCH_3)(CO)_9$ has been reported.[27] The reaction forming **3a** may proceed via a mixed species such as "$CoFe_2(\mu\text{-}COCH_3)(CO)_{9/10}$" involving sequential replacement of iron atoms giving the final product. However, no mixed Fe–Co complexes were isolated, the only other products detected being $Fe(CO)_5$ and $Co_4(CO)_{12}$.

Although crystal structures of several similar molecules have been reported including the close analogues **3b**, R = H,[28] and **3c**, R = CH_3,[29] complex **3a** was studied by X-ray crystallography to provide information about the interaction of the C_{3v} "$Co_3(CO)_9$" fragment with the nonaxially symmetric methoxymethylidyne ligand. Complexes **3b** and **3c** retain the effective threefold axial symmetry of the cluster fragment.

The molecular structure and atomic labeling of complex **3a** are shown in Figure 1, with a stereoview in Figure 2 clearly showing the disposition of the μ_3-$COCH_3$ ligand. Atomic coordinates are given in Table I, with selected metrical parameters in Table II. The well-established stereochemical features common to **3a**, **3b**,[28] and **3c**[29] will not be discussed here. The three Co–Co separations are identical within error (average Co–Co = 2.479 [1] Å) and exactly equivalent to those reported[28] for **3b** (2.479 [7] Å) in an accurate neutron diffraction study at 102 K. However, the $Co–C_{alkylidyne}$ bond lengths, identical within error in **3b** (Co–C = 1.893 (1), 1.894 (1), and 1.895 (1) Å),[28] are

Table II. Selected Bond Lengths (Å) and Bond Angles (deg) with Estimated Standard Deviations in Parentheses for $Co_3(\mu_3\text{-}COCH_3)(CO)_9$ (3a)

Bond Lengths			
Co(1)–Co(2)	2.478 (1)	Co(1)–C(1)	1.786 (3)
Co(1)–Co(3)	2.478 (1)	Co(1)–C(2)	1.800 (3)
Co(2)–Co(3)	2.480 (1)	Co(1)–C(3)	1.832 (3)
Co(1)–C(10)	1.882 (2)	Co(2)–C(4)	1.823 (3)
Co(2)–C(10)	1.912 (2)	Co(2)–C(5)	1.784 (3)
Co(3)–C(10)	1.906 (2)	Co(2)–C(6)	1.782 (3)
C(10)–O(10)	1.320 (3)	Co(3)–C(7)	1.788 (3)
C(11)–O(10)	1.419 (4)	Co(3)–C(8)	1.787 (3)
C(11)–H(1)	0.91 (4)	Co(3)–C(9)	1.825 (3)
C(11)–H(2)	1.08 (3)		
C(11)–H(3)	0.98 (4)	C–O(carbonyl)	1.126 [1][a]
Bond Angles			
Co(2)–Co(1)–Co(3)	60.0 (1)	Co(1)–C(10)–O(10)	126.9 (2)
Co(1)–Co(2)–Co(3)	60.0 (1)	Co(2)–C(10)–O(10)	133.3 (2)
Co(1)–Co(3)–Co(2)	60.0 (1)	Co(3)–C(10)–O(10)	133.0 (2)
C_{eq}–Co–C_{eq}	96.5 [1][a]	Co–C–O(carbonyl)	178.8 [1][a]
C_{eq}–Co–C_{ax}	102.3 [1][a]		
Co(1)–C(10)–Co(2)	81.6 (1)	C(10)–O(10)–C(11)	118.6 (2)
Co(1)–C(10)–Co(3)	81.7 (1)		
Co(2)–C(10)–Co(3)	81.0 (1)		

[a] Mean value.

no longer so in **3a**. Thus the unique Co–C separation Co(1)–C(10) is 1.882 (2) Å, significantly shorter than the Co(2)–C(10) and Co(3)–C(10) vectors (1.912 (2) and 1.906 (2) Å, respectively), which are themselves equivalent within error. This is a reflection of the orientation of the $COCH_3$ group in **3a** essentially perpendicular to the Co(2)–Co(3) bond (the normal to the plane C(10)O(10)C(11) is at an angle of 0.63° to the Co(2)–Co(3) vector), which reduces the symmetry from C_{3v} as found in **3b** and **3c** to C_s in complex **3a**. The methyl hydrogen atomic positions, determined from a difference Fourier and subject to unrestricted refinement, also comply with the molecular mirror symmetry. Thus the deviations of H(2), H(1), and H(3) from the mirror plane defined by Co(1)C(10)O(10)C(11) are −0.04 (3), 0.79 (3), and −0.80 (3) Å, respectively.

The Co–C distances associated with the carbonyl groups trans to the $COCH_3$ ligand, average Co–C = 1.827 [2] Å, are significantly greater than those cis, average Co–C = 1.788 [3] Å, and may be compared with the corresponding values found for **3b** of 1.837 [2] and 1.796 [2] Å (X-ray study at 92 K).[28] These differences are indicative of the strong π-acidity of the alkylidyne ligand,[2,10,30] resulting in competition for π-electron density. Finally it is interesting to note that the C(10)–O(10) vector is not perpendicular to the Co_3 triangle but is tipped toward the unique cobalt atom Co(1). This is evidenced by the Co(1)–, Co(2)–, and Co(3)–C(10)–O(10) angles (126.9 (2), 133.3 (2), and 133.0 (2)°, respectively). A similar distortion is observed[31] in the related acetoxytricobalt methylidyne complex $Co_3(\mu_3\text{-}COC(O)CH_3)(CO)_9$ and may be due to nonbonded interactions of the methyl hydrogen atoms with the carbonyl ligands C(5)–O(5) and C(8)–O(8).

The tricobalt alkylidyne complexes $Co_3(\mu_3\text{-}CR)(CO)_9$ (**3**) are paradigm molecules for the symmetric μ_3-CR bonding mode and have received widespread attention over a period of years.[32] There has been a recent resurgence of interest

(24) Seyferth, D.; Hallgren, J. E.; Hung, P. L. K. *J. Organomet. Chem.* **1973**, *50*, 265.
(25) Blumhofer, R.; Fischer, K.; Vahrenkamp, H. *Chem. Ber.* **1986**, *119*, 194.
(26) Jeffery, J. C.; Lewis, D B.; Lewis, G. E.; Stone, F. G. A. *J. Chem. Soc., Dalton Trans.* **1985**, 2001.
(27) Fischer, E. O.; Dänveritz, A. *Angew. Chem., Int. Ed. Engl.* **1975**, *14*, 346.
(28) Leung, P.; Coppens, P.; McMullan, R. K.; Koetzle, T. F. *Acta Crystallogr., Sect. B: Struct. Crystallogr. Cryst. Chem.* **1981**, *B37*, 1347.
(29) Sutton, P. W.; Dahl, L. F. *J. Am. Chem. Soc.* **1967**, *89*, 261.
(30) Dalton, D. M.; Barnett, D. J.; Duggan, T. R.; Keister, J. B.; Malik, P. T.; Modi, S. P.; Shaffer, M. R.; Smesko, S. A. *Organometallics* **1985**, *4*, 1854.
(31) Bätzel, V.; Schmid, G. *Chem. Ber.* **1976**, *109*, 3339.
(32) (a) Seyferth, D. *Adv. Organomet. Chem.* **1976**, *14*, 97. (b) Penfold, B. R.; Robinson, B. R. *Acc. Chem. Res.* **1973**, *6*, 73. (c) Palyi, G.; Placenti, F.; Marko, L. *Inorg. Chim. Acta Rev.* **1970**, *4*, 109. (d) Schmid, G. *Angew. Chem., Int. Ed. Engl.* **1978**, *17*, 392.

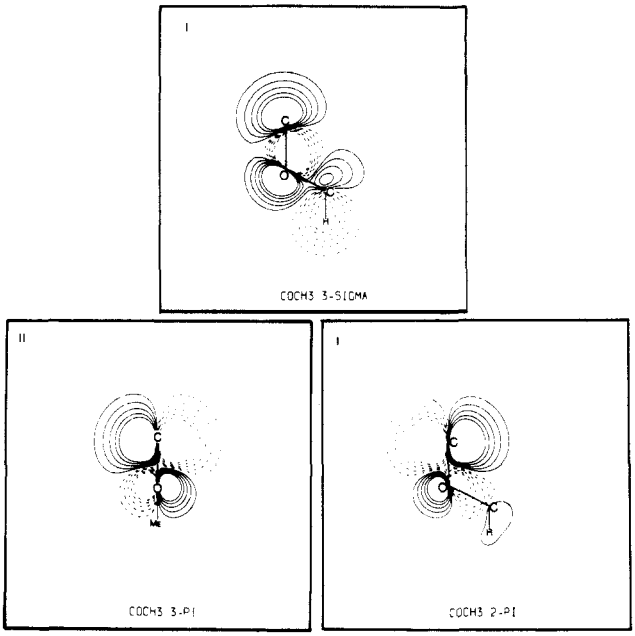

Figure 3. Contour plots of the frontier orbitals of $COCH_3$ fragment: view 1, in plane of ligand; view II, perpendicular to ligand plane through CO bond.

in their detailed electronic structure as evidenced by the PES studies of Granozzi et al.[33] (R = H, F, Cl, Br, I, CH_3, CF_3, $COOCH_3$), Hall and Chesky[34] (R = H, Cl, Br, I, CH_3, OCH_3), Fehlner and co-workers[35] (R = CH_3), and Jolly et al.[16] (R = $SiEt_3$, H, CH_3, Br, Cl, NMe_2, OCH_3). Molecular orbital calculations on **3** have also been reported by the groups of Hoffmann[36] (R = H), Fehlner[35] (R = CH_3), and Hall[34] (R = Cl). Although Fenske–Hall MO calculations were carried out[34] on **3a**, R = OCH_3, no details were reported. An EHMO study on **3a** was thus undertaken, analyzing the molecule in terms of the C_{3v} fragment "$Co_3(CO)_9$" and the $COCH_3$ moiety. The general bonding pattern emerging is in essential agreement with the previous studies,[34,36] and only salient points of interest will be discussed.

Contour plots of the frontier orbitals of the $COCH_3$ fragment, which are important in bonding to the cluster, are shown in Figure 3. The 3σ-donor orbital is well-hybridized at the alkylidyne carbon to act as an effective σ-donor and also constitutes the "lone pair" on the oxygen atom. The 2π and 3π levels are descended from the π^* set of CO, are C–O antibonding, and due to the bent disposition of the $COCH_3$ ligand are no longer degenerate. However, the separation is small (ca. 0.14 eV) and only provides a tiny barrier of 5 kJ mol^{-1} to the rotation of the $COCH_3$ group about the Co_3 triangle, with the calculated minimum lying at the observed geometry.

The 2π and 3π levels of $COCH_3$ are considerably more stable than the corresponding π^* orbitals of CO and, lying close in energy to the cluster-based e set of donor orbitals, imply that $COCH_3$ is a strong π-acid. A similar conclusion about the π-acidity of alkylidyne ligands has been reached by Kostič and Fenske[37] in MO studies on mononuclear species. The interactions of 2π and 3π with the donor e set (2e in the Hoffmann study[36]) and that of the symmetric $2a_1$ cluster acceptor orbital[36] with 3σ (and also with another low-lying σ-donor orbital not illustrated here) provide some 67% of the total overlap population between the fragments, implying these interactions form the major component of the bonding of the $COCH_3$ ligand to the tricobalt cluster moiety.

Table III. Calculated Atomic Charges for $Co_3(\mu_3\text{-CR})(CO)_9$

atom	R = H	R = OCH_3	R = CH_3	R = CH_3[a]
Co	−0.132	−0.180, −0.164	−0.140	−0.131
C_{alk}	−0.398	−0.142	−0.398	−0.301
C_{eq}	0.316	0.317	0.310	0.147
O_{eq}	−0.211	−0.227	−0.216	−0.048
C_{ax}	0.245	0.249	0.247	0.087
O_{ax}	−0.210	−0.214	−0.213	−0.044

[a] Fenske–Hall calculations taken from ref 35.

The Mulliken overlap populations between the cobalt atoms and alkylidyne carbon, 0.477 between Co(1) and C(10) and 0.470 between Co(2), Co(3) and C(10), suggests a very marginally stronger bond between Co(1) and C(10) as is experimentally observed. However, the observed differences in the cobalt–carbonyl carbon separations are not mirrored in the overlap populations that are 0.722 for the Co–C_{eq} and 0.760 for the Co–C_{ax} interactions.

Table III shows the results of self-consistent charge-iterative calculations on **3**, R = H, CH_3, and OCH_3, with previously reported values for R = CH_3 (derived from Fenske–Hall calculations[35]), quoted for comparison. The agreement between the EHMO and Fenske–Hall methods is reasonable, especially as regards the charges on the cobalt and alkylidyne carbon centers, and illustrates a consistent electron-rich character for the alkylidyne carbon atom, as previously noted in theoretical[35] and deformation density[38] studies. This is in line with ideas that the observed low-field ^{13}C NMR chemical shift of the alkylidyne carbon in these systems[39] cannot be ascribed to deshielding through a positive charge at that atom.[40] Interestingly for R = OCH_3, the negative charge on the alkylidyne carbon is noticeably *less* than that for R = H or CH_3, suggesting that any charge redistribution due to π donation from the alkoxy oxygen is not responsible for reducing the electron deficiency at this carbon. Canonicals such as I or II are often drawn[2,15,16] to represent the bonding in methoxymethylidyne complexes, but the high negative charge calculated for the alkoxy oxygen (−0.34) implies that II may be somewhat unrealistic.

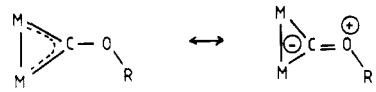

I II

We have previously reported[11] that reaction of $Fe_3(\mu\text{-H})(\mu\text{-}COCH_3)(CO)_{10}$ with $[Ni(\mu\text{-CO})(\mu\text{-}C_5H_5)]_2$ gave three products, one of these being the new methoxymethylidyne complex $Fe_3(\mu_3\text{-}COCH_3)(\mu\text{-CO})_2(CO)_6(\eta\text{-}C_5H_5)$ (**4**). In view of the varying degrees of semi-μ_3-bridging interactions of the $COCH_3$ ligand in trinuclear clusters previously demonstrated,[11,12] it was of some interest to investigate the structure of **4**. This complex possesses a less symmetric albeit homometallic trinuclear cluster template and should

(33) Granozzi, G.; Tondello, E.; Ajó, D.; Casarin, M.; Aime, S.; Osella, D. *Inorg. Chem.* **1982**, *21*, 1081.
(34) Chesky, P. T.; Hall, M. B. *Inorg. Chem.* **1981**, *20*, 4419.
(35) De Kock, R. L.; Wong, K. S.; Fehlner, T. P. *Inorg. Chem.* **1982**, *21*, 3203.
(36) Schilling, B. E. R.; Hoffmann, R *J. Am. Chem. Soc.* **1979**, *101*, 3456.
(37) Kostič, N. M.; Fenske, R. F. *J. Am. Chem. Soc.* **1981**, *103*, 4677.
(38) Leung, P.; Holladay, A.; Coppens, P. *Acta Crystallogr., Sect. A: Found. Crystallogr.* **1983**, *A39*, 377.
(39) (a) Seyferth, D.; Williams, G. H.; Eschbach, C. S.; Nestle, M. O.; Merold, J. S.; Hallgren, J. F. *J. Am. Chem. Soc.* **1979**, *101*, 4867. (b) Aime, S.; Milone, L.; Valle, M. *Inorg. Chim. Acta* **1976**, *18*, 9.
(40) Fenske, R. F. In *Organometallic Compounds*; Shapiro, B. L., Ed.; Texas A&M University Press: College Station, TX, pp 305–333.

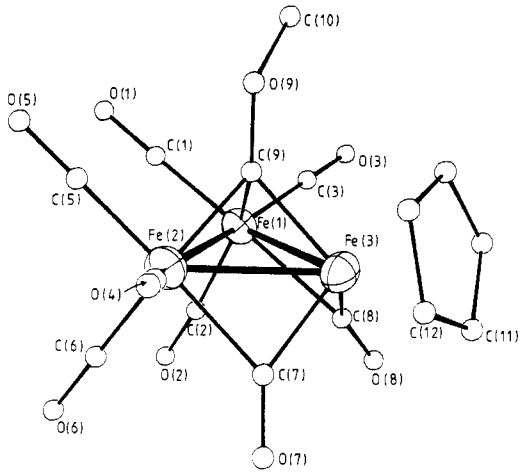

Figure 4. Molecular geometry and atomic labeling scheme for the complex $Fe_3(\mu_3\text{-}COCH_3)(\mu\text{-}CO)_2(CO)_6(\eta\text{-}C_5H_5)$ (**4**).

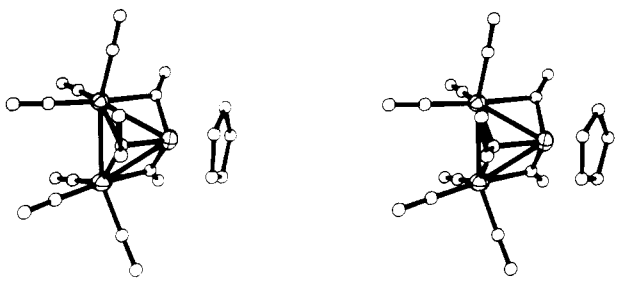

Figure 5. Stereoview of $Fe_3(\mu_3\text{-}COCH_3)(\mu\text{-}CO)_2(CO)_6(\eta\text{-}C_5H_5)$ (**4**) showing orientation of $COCH_3$ group.

provide a useful contrast to the highly symmetric C_{3v} framework of complex **3a**.

The molecular structure of complex **4** is shown in Figure 4, with a stereoview illustrating the orientation of the $COCH_3$ ligand in Figure 5. Positional parameters are given in Table IV and important metrical parameters in Table V. The cluster fragment "$Fe_3(\mu\text{-}CO)_2(CO)_6(\eta\text{-}C_5H_5)$" has approximate mirror symmetry, although the iron–iron vectors are not exactly equivalent (Fe(1)–Fe(2) = 2.582 (1), Fe(1)–Fe(3) = 2.547 (1), and Fe(2)–Fe(3) = 2.524 (1) Å). In contrast to the situation found in complex **3a**, the C–O–C plane of the $COCH_3$ ligand is not perpendicular to a metal–metal bond but lies essentially *parallel* to the Fe(1)–Fe(2) vector. The angle between the mean plane C(9)–O(9)–C(10) and the Fe(1)–Fe(2) bond is 0.39°. This alternative geometry to that observed for **3a** also allows optimization of the π overlap between the $COCH_3$ group and the cluster framework. The overall ligand geometry in **4** is very similar to that found[41] in the μ_3-propylidyne complex $Fe_3(\mu_3\text{-}CC_2H_5)(\mu\text{-}CO)_2(CO)_6\{\eta\text{-}C_5H_2(CH_3)_2(C_2H_3)\}$ (**5**), synthesized by reaction of $Fe_3(CO)_{12}$ with $CH_3C{\equiv}CH$. The ethyl group orientation relative to the Fe_3 triangle observed in **5** is presumably determined solely by nonbonded contacts and packing forces.

The $Fe\text{–}C_{alkylidyne}$ separations Fe(1)–C(9) = 1.905 (5), Fe(2)–C(9) = 1.935 (5), and Fe(3)–C(9) = 1.952 (5) Å in **4** indicate that the $COCH_3$ ligand forms an essentially symmetric μ_3 bridge, though as in **3a** there is some minor asymmetry. The μ-carbonyl ligands form asymmetric bridges with Fe(3)–C(7) = 1.869 (5), Fe(2)–C(7) = 2.051 (5) Å and Fe(3)–C(8) = 1.828 (5), Fe(1)–C(8) = 2.148 (5) Å; similar values are found[41] for **5**. The α values[42] are 0.097 and 0.175 for C(7)–O(7) and C(8)–O(8), respectively. The cyclopentadienyl ligand is tilted up toward the $COCH_3$ group, with an angle of 21.1° between Fe(3)–CT and the Fe_3 plane (CT = centroid of C_5 ring).

Symmetric μ_3-$COCH_3$ bridges have been found in the complexes $Au_nRu_3(\mu\text{-}H)_{3-n}(\mu_3\text{-}COCH_3)(CO)_9(PPh_3)_n$ (n = 1,[10] 2,[9] 3[10]), $Fe_3Pt(\mu_3\text{-}H)(\mu_3\text{-}COCH_3)(CO)_{10}(PPh_3)$,[8] $Ru_3(\mu\text{-}H)(\mu_3\text{-}COCH_3)(CO)_8(1,3\text{-}C_6H_8)$,[43] $[Fe_4(\mu_3\text{-}COCH_3)(\mu\text{-}CO)(CO)_{11}]^-$,[6b,44] $Fe_2Ni(\mu_3\text{-}COCH_3)(\mu_3\text{-}CO)(CO)_6(\eta\text{-}C_5H_5)$,[11]

Table IV. Atomic Positional (Fractional Coordinate) Parameters with Estimated Standard Deviations in Parentheses for the Complex $Fe_3(\mu_3\text{-}COCH_3)(\mu\text{-}CO)_2(CO)_6(\eta\text{-}C_5H_5)$ (4)

	x/a	y/b	z/c
Fe(1)	0.57786 (6)	0.12302 (3)	0.77039 (6)
Fe(2)	0.84086 (7)	0.07557 (3)	0.81787 (7)
Fe(3)	0.74491 (7)	0.13538 (3)	0.59374 (6)
C(1)	0.5778 (5)	0.1397 (2)	0.9463 (5)
C(2)	0.4833 (5)	0.0392 (3)	0.7732 (5)
C(3)	0.4317 (5)	0.1830 (2)	0.7179 (4)
C(4)	1.0285 (6)	0.0736 (3)	0.8058 (6)
C(5)	0.8858 (6)	0.1026 (3)	0.9925 (6)
C(6)	0.7877 (6)	−0.0140 (3)	0.8523 (5)
C(7)	0.8088 (5)	0.0419 (3)	0.6189 (5)
C(8)	0.5612 (5)	0.0989 (2)	0.5571 (5)
C(9)	0.7606 (5)	0.1694 (2)	0.7811 (4)
C(10)	0.7199 (6)	0.2885 (2)	0.8444 (5)
C(11)	0.7618 (11)	0.1471 (4)	0.3891 (6)
C(12)	0.8986 (9)	0.1454 (4)	0.4665 (8)
C(13)	0.9132 (7)	0.2021 (4)	0.5510 (6)
C(14)	0.7895 (9)	0.2395 (3)	0.5304 (7)
C(15)	0.6886 (7)	0.2065 (5)	0.4332 (9)
O(1)	0.5760 (4)	0.1520 (2)	1.0592 (4)
O(2)	0.4237 (5)	−0.0122 (2)	0.7856 (4)
O(3)	0.3354 (5)	0.2199 (2)	0.6851 (4)
O(4)	1.1489 (5)	0.0745 (33)	0.7967 (5)
O(5)	0.9168 (5)	0.1201 (3)	1.1031 (4)
O(6)	0.7540 (5)	−0.0701 (2)	0.8741 (5)
O(7)	0.8313 (4)	−0.0101 (2)	0.5616 (4)
O(8)	0.4649 (4)	0.0780 (2)	0.4779 (4)
O(9)	0.8162 (3)	0.2297 (2)	0.8362 (3)

Table V. Selected Bond Lengths (Å) and Bond Angles (deg) with Estimated Standard Deviations in Parentheses for $Fe_3(\mu_3\text{-}COCH_3)(\mu\text{-}CO)_2(CO)_6(\eta\text{-}C_5H_5)$ (4)

Bond Lengths

Fe(1)–Fe(2)	2.582 (1)	Fe(1)–C(9)	1.905 (5)
Fe(1)–Fe(3)	2.547 (1)	Fe(2)–C(9)	1.935 (5)
Fe(2)–Fe(3)	2.524 (1)	Fe(3)–C(9)	1.952 (5)
Fe(1)–C(1)	1.776 (6)	Fe(2)–C(4)	1.776 (6)
Fe(1)–C(2)	1.816 (5)	Fe(2)–C(5)	1.790 (6)
Fe(1)–C(3)	1.784 (5)	Fe(2)–C(6)	1.812 (6)
Fe(1)–C(8)	2.148 (5)	Fe(2)–C(7)	2.051 (5)
Fe(3)–C(7)	1.869 (5)		
Fe(3)–C(8)	1.828 (5)	Fe(3)–C_{cp}	2.095 [4][a]
C–O(carbonyl)	1.147 [7][a]	Cp C–C	1.37 [1][a]
C(9)–O(9)	1.332 (6)	C(10)–O(9)	1.439 (6)

Bond Angles

Fe(2)–Fe(1)–Fe(3)	59.0 (1)	Fe(1)–C(9)–Fe(2)	84.5 (2)
Fe(1)–Fe(2)–Fe(3)	59.8 (1)	Fe(1)–C(9)–Fe(3)	82.6 (2)
Fe(1)–Fe(3)–Fe(2)	61.2 (1)	Fe(2)–C(9)–Fe(3)	81.0 (2)
Fe(1)–C(8)–O(8)	131.4 (4)	Fe(2)–C(7)–Fe(3)	80.0 (2)
Fe(3)–C(8)–O(8)	149.1 (4)	Fe(2)–C(7)–O(7)	136.1 (4)
Fe(1)–C(8)–Fe(3)	79.2 (2)	Fe(3)–C(7)–O(7)	143.8 (5)
Fe(1)–C(9)–O(9)	134.5 (4)	C(9)–O(9)–C(10)	118.6 (4)
Fe(2)–C(9)–O(9)	126.5 (4)		
Fe(3)–C(9)–O(9)	129.5 (4)	Fe–C–O(carbonyl)	178.9 [2][a]

[a] Mean value.

(41) Aime, S.; Milone, L.; Sappa, E.; Tiripicchio, A. *J. Chem. Soc., Dalton. Trans.* **1977**, 227.

(42) Curtis, M. D.; Han, K. R.; Butler, W. M. *Inorg. Chem.* **1980**, *19*, 2096.

(43) Churchill, M. R.; Beanan, L. R.; Wasserman, H. J.; Bueno, C.; Rahman, Z. A.; Keister, J. B. *Organometallics* **1983**, *2*, 1179.

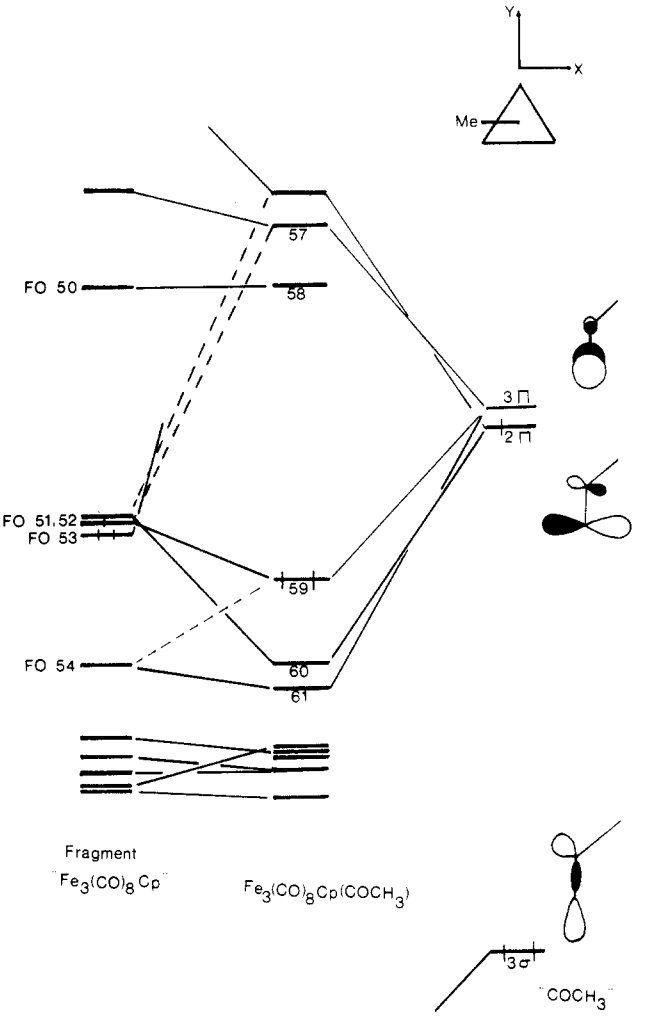

Figure 6. Orbital interaction diagram between the fragments $COCH_3$ and $Fe_3(\mu\text{-}CO)_2(CO)_6(\eta\text{-}C_5H_5)$.

$Fe_3(\mu_3\text{-}CCH_3)(\mu_3\text{-}COCH_3)(CO)_9$,[45] and $Fe_3(\mu_3\text{-}Bi)(\mu_3\text{-}COCH_3)(CO)_9$,[53] while asymmetric "semi-μ_3"interactions are observed in $Fe_2M(\mu_3\text{-}COCH_3)(\mu\text{-}H)(CO)_7(\eta\text{-}C_5H_5)$ (M = Co,[11] Rh[12]). A partial understanding of the "semi-μ_3" character in the latter complexes is afforded[12] by examination of the nature and localization of the π-donor and σ-acceptor orbitals of the cluster fragment "$Fe_2M(\mu\text{-}H)(CO)_7(\eta\text{-}C_5H_5)$".

Figure 6, an interaction diagram between the C_s fragment "$Fe_3(\mu\text{-}CO)_2(CO)_6(\eta\text{-}C_5H_5)$" and $COCH_3$, show the results of a similar EHMO analysis on complex **4**. Since the relevant fragment orbitals (FO'S) are complex functions of the iron atom basis sets, orbital contour plots of the FO's 51–54 are illustrated in Figure 7. The σ-acceptor FO 53 has maximum overlap with $COCH_3$ 3σ above the centroid of the Fe_3 triangle, i.e. favors an equal interaction with all three iron atoms. The in-phase combination of FO 53 and 3σ is strongly stabilized. FOs 51 and 52 are clearly of π symmetry (a'' and a', respectively) relative to the Fe_3 centroid and provide a match for the 2π and 3π levels of $COCH_3$. The HOMO MO 59 derives from the in-phase combination of FO 52 and 3π, with out of phase mixing in of FO 54 (also of a' symmetry). FO 54 has significant overlap with 3π, but the poorer energy match

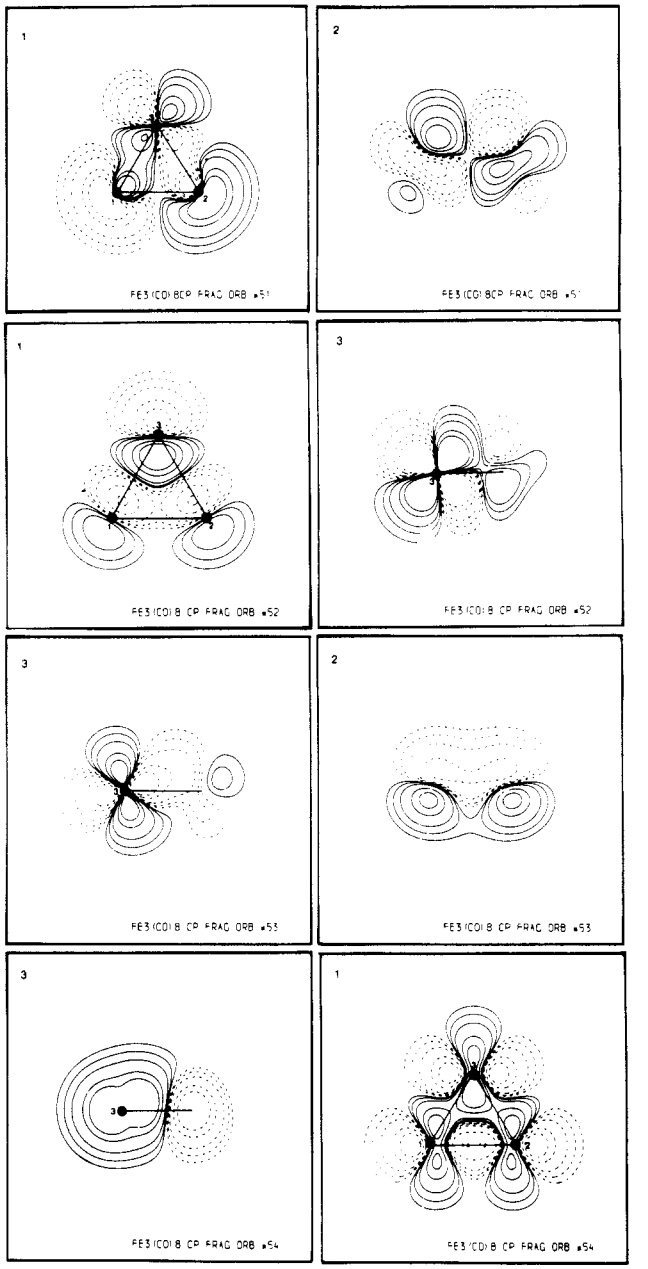

Figure 7. Contour plots of the fragment orbitals 51–54 of $Fe_3(\mu\text{-}CO)_2(CO)_6(\eta\text{-}C_5H_5)$: view 1, parallel to and 0.5 Å above Fe_3 plane; view 2, parallel to Fe(1)–Fe(2) and perpendicular to Fe_3 plane through centroid; view 3, perpendicular to Fe_3 plane and Fe(1)–Fe(2) through Fe(3).

results in only slight stabilization (giving rise to MO 61). MO 60 is composed of the corresponding interaction of FO 51 and 2π. A lower lying nest of Fe 3d based cluster fragment orbitals are essentially unperturbed by interaction with the $COCH_3$ moiety. The LUMO MO 58 has no alkylidyne character and is primarily composed of FO 50, an in-plane Fe–Fe σ-antibonding orbital. A similar orbital is also the LUMO in the tricobalt nonacarbonyl alkylidyne complexes **3**.[36] MO's 57 and 56 however have some alkylidyne carbon character (7% and 13%, respectively) and are descended mainly from higher lying FO's with some admixture of FO 51 and FO 52.

The interactions of FO's 51 and 52 with 2π and 3π and FO 53 and 3σ (and also with a lower lying σ-donor orbital not shown) account for 65% of the total overlap population between the fragments "$Fe_3(\mu\text{-}CO)_2(CO)_6(\eta\text{-}C_5H_5)$" and $COCH_3$, and so constitute the major component of their bonding. The FO's of π symmetry, 51 and 52, are nearly

(44) Holt, E. M.; Whitmire, K.; Shriver, D. F. *J. Chem. Soc., Chem. Commun.* **1980**, 778.
(45) Wong, W.-K.; Chiu, K. W.; Wilkinson, G.; Galas, A. M. R.; Thornton-Pett, M.; Hursthouse, M. *J. Chem. Soc., Dalton Trans* **1983**, 1557.

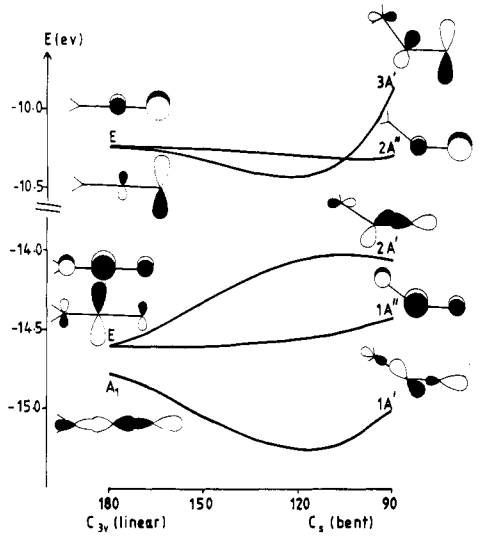

Figure 8. Correlation diagram for the $COCH_3$ ligand.

degenerate and resemble the e donor set of "$Co_3(CO)_9$".[36] The alkylidyne bonding in the two molecules **3a** and **4** is thus closely analogous.

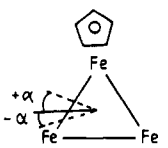

The barrier to rotation of the $COCH_3$ moiety about the cluster framework in **4** however presents a different situation to that for **3a**. With the cyclopentadienyl group tilted 21.1° toward the $COCH_3$ ligand (as crystallographically observed), rotation of the methyl group about the C–O bond brings about unacceptably close contacts as α approaches +90° (methyl–H···Cp–H distances of ca. 1.2 Å). This results in a high barrier in excess of 350 kJ mol^{-1} (depending on the exact rotational orientation of the Cp group). On the other hand rotation toward α = –90° results in a shallow barrier of only ca. 10 kJ mol^{-1}. ^{13}C NMR evidence is in favor of a small barrier, since line widths of the signals due to the two apparently equivalent $Fe(CO)_3$ groups in **4** are still narrow at –60 °C.[11] Reducing the tilt angle of the cyclopentadienyl group rapidly alleviates this high barrier; with the Cp ligand perpendicular to the Fe_3 triangle it is only ca. 47 kJ mol^{-1}. The barrier to rotation of the $COCH_3$ group is thus dominated by steric rather than electronic factors. The calculated minimum lies at an α angle of +11°, in reasonable agreement with the observed geometry.

The other posited mode of fluxionality of the $COCH_3$ group is via inversion at the central oxygen.[3] Calculations on **4** and other similar molecules surprisingly indicate that a linear C–O–CH_3 geometry is 40 kJ mol^{-1} *more stable* than the bent form, in contradiction to experimental observation. Thus for **4** the C(9)–O(9)–C(10) angle is 118.6 (4)° with a corresponding angle of 118.6 (2)° for **3a**. From a number of accurate X-ray studies on methoxymethylidyne compounds[2,9–13,43,45] a mean value of 119.3 [2]° is calculated, with little variation from this average value (reported range 115.6 (9)[10]–122.5 (9)°[13]).

A correlation diagram for the $COCH_3$ ligand, derived from EHMO calculations, is shown in Figure 8. It is closely similar to that of the well-known polyatomic HAB type.[46] As the C–O–C angle is reduced from 180° the in-plane π-bonding orbital rises in energy due to loss of π overlap and mixes with σ A_1 to become the σ-donor frontier orbital 2A′ (3σ in Figure 3). The out-of-plane component of the E antibonding set is barely affected by bending, becoming 2A″ (3π), while the in-plane π^* orbital 3A′ (2π) is slightly reduced in energy resulting in a shallow minimum at 120°. Further reduction of the C–O–C angle results in a steep rise in energy of this orbital due to loss of π overlap and partly due to interaction with 2A′. The 3A′ is singly occupied in the neutral hypothetical $COCH_3$, an 11-electron fragment. Interactions of $COCH_3$ with the cluster fragments discussed above will lead to population of both 2A″ and 3A′ and regardless of the exact extent should result in a preferred C–O–C geometry of ca 120°. The σ-donor orbital 2A′ (3σ) is expected to be partially depopulated on complexation, and it may be that the parameterization used in the calculations above does not adequately reflect the synergic interplay between σ donation and π acceptance.

The unit $COCH_3^+$ is isoelectronic with $CNCH_3$, and due to the greater electronegativity of oxygen, it is expected to be a better π acceptor. The π-acidity of $CNCH_3$ as a function of the angle at nitrogen has been studied by Howell et al. using ab initio methods.[47] They conclude that the π-acceptor ability increases substantially on bending. A similar, though not as marked stabilization of a π^* level (3A′) of $COCH_3$, leading to enhanced π-acidity on bending, is observed in our EHMO study. Isocyanide ligands are known to bend when extensive π-back-donation occurs,[47–49] though angles as small as those observed in methoxymethylidyne complexes are rather rare (e.g. 123 (1)° as found in $Fe_2(\mu\text{-CNEt})_3(CNEt)_6$[48]). The "windshield wiper" mode of fluxional inversion at the N atom of bridging isocyanides is commonly proposed,[48,49] and our EHMO calculations imply that a similar mechanism involving the methoxymethylidyne ligand should be borne in mind, particularly when steric factors mitigate against free rotation about the C–O bond.

Shapley has demonstrated that the methoxymethylidyne ligand in $Os_3(\mu\text{-H})(\mu\text{-CR})(CO)_{10}$ (**2b**, R = OCH_3) can be functionalized by sequential treatment with a nucleophile and electrophile to give the complexes **2a**, R = H,[17] and **2c**, R = Ph.[20] Another derivative (**2d**, R = CH_2CHMe_2) has been prepared by Green et al.[50] via a different route. These complexes display an interesting "semi-μ_3" alkylidyne bonding mode, where the angle between the Os_3 and $\overline{Os(\mu\text{-C})Os}$ planes is acute rather than obtuse as observed in other $Os_3(\mu\text{-H})(\mu\text{-X})(CO)_{10}$ complexes.[51] The corresponding interplanar angle in **2b** is presumably slightly greater than 90°, as judged by the related triphenylphosphine aurio derivative $Os_3(\mu\text{-AuPPh}_3)(\mu\text{-COCH}_3)(CO)_{10}$ (average 103 (1)°)[13] and the iron (91.1°)[1] and ruthenium (94.9°)[43] analogues. It has been suggested that the driving force for this "semi-μ_3" interaction in **2a**, **2c**, and **2d** is electron donation from the saturated 18e $Os(CO)_4$ unit to the electrophilic alkylidyne carbon center and that the π-donor ability of the methoxy substituent in **2b** al-

(46) Gimarc, B. M. *J. Am. Chem. Soc.* **1971**, *93*, 815.

(47) Howell, J. A. S.; Saillard, J.-Y.; Le Beuze, A.; Jaouen, G. *J. Chem. Soc., Dalton Trans.* **1982**, 2533.

(48) Bassett, J. M.; Barker, G K.; Green, M.; Howard, J. A. K.; Stone, F. G. A.; Wolsey, C. *J. Chem. Soc., Dalton Trans.* **1981**, 219 and references therein.

(49) Cotton, F. A.; Frenz, B. A. *Inorg. Chem.* **1974**, *13*, 153.

(50) Green, M.; Orpen, A. G.; Shaverien, C. *J. Chem. Soc., Chem. Commun.* **1984**, 37.

(51) (a) Churchill, M. R.; Wasserman, H. J. *Inorg. Chem.* **1981**, *20*, 2905 and references therein. (b) Deeming, A. J. *Adv. Organomet. Chem.*, in press.

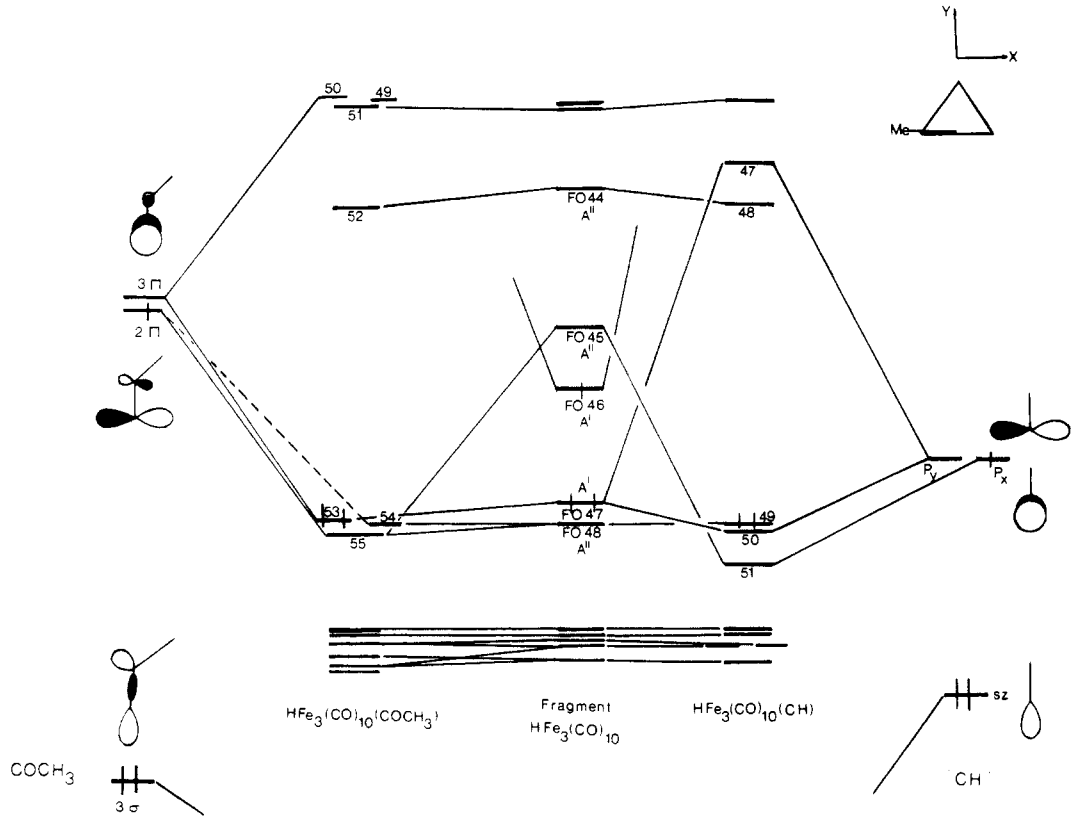

Figure 9. Orbital interaction diagram between the fragments $Fe_3(\mu\text{-H})(CO)_{10}$ and CH and $COCH_3$.

leviates electron deficiency at this center and hence reduces the "semi-μ_3" interaction.[17]

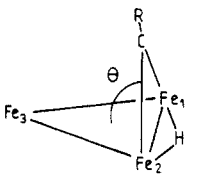

In an effort to understand this unusual interaction EHMO calculations have been carried out on the model molecules $Fe_3(\mu\text{-H})(\mu\text{-CR})(CO)_{10}$ (**1a**, R = OCH_3, and **1b**, R = H). Although **1b** has been briefly reported,[52] no structural details are available. The interaction diagram shown in Figure 9 is calculated with the CR fragment perpendicular both to the Fe(1)–Fe(2) vector and the triiron triangle (i.e. orthogonal geometry) and for **1a** with the C–O–C plane parallel to Fe(1)–Fe(2). In the crystal structures the interplanar angle θ is 91.1° for **1a**[1] and 69.7° for **2b**.[17] The frontier orbitals of the alkylidyne moiety CR are well-known[36,37] and for CH consist of a σ-donor sz hybrid and a degenerate pair of p_x, p_y orbitals as π acceptors. Contour plots for the four important cluster fragment orbitals FO's 45–48 are shown in Figure 10. The bonding picture is similar to the above discussed complexes in that one σ- and two π-type interactions are important. The σ acceptor FO 46 is highly localized on Fe(1) and Fe(2) such that greatest overlap with either 3σ of "$COCH_3$" or the sz hybrid of "CH" occurs in the orthogonal geometry.

Two types of deformations leading to increased "semi-μ_3" interactions can be envisaged. In type I the CR unit is tilted such that the CR vector is still perpendicular to Fe(1)–Fe(2) (i.e., Fe(1)–Fe(2)–C–R are coplanar) while for type II the CR vector remains orthogonal to the triiron triangle. This latter equilibrium geometry is generally

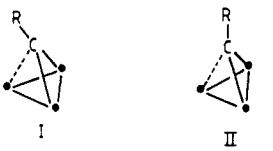

found in μ_3-alkylidyne complexes, e.g. $Co_3(\mu\text{-CR})(CO)_9$,[28,29] and is the favored orientation for these type of molecules. The experimental evidence vis-à-vis the "semi-μ_3" interaction is less clear-cut. Thus for $Os_3(\mu\text{-H})(\mu\text{-CR})(CO)_{10}$ (R = Ph), the $C\text{–}C_{phenyl}$ axis is virtually perpendicular to the triosmium plane (angle between C(1)–C(2) and the normal to Os_3 plane = 0.49°[20]), while for R = H, the methylidyne unit appears tilted out of the $\overline{Os(\mu\text{-C})Os}$ plane by ca. 24.5° *toward* the unique Os center.[17]

Steric interactions between the "semi-μ_3" alkylidyne ligand and the carbonyl ligands on the $Os(CO)_4$ group perturb the normal[51] geometry of this unit and cause a rotation about the Os atom away from the alkylidyne, a feature of these complexes previously discussed by Shapley, Churchill, et al.[20] This perturbation is particularly severe in $Os_3(\mu\text{-H})(\mu_3\text{-CPh})(CO)_9(\eta^1\text{-C(OMe)}_2)$.[19] We have analyzed the deformations in the molecules **1a** and **1b** in terms of a type II mode, since calculations on **1b** indicate this geometry is at lower energy, due principally to the minimization of nonbonded interactions.

The σ interaction involving FO 46 is destabilized by significant movement of the CR ligand toward the centroid of the triangle, due to loss of overlap and introduction of Fe(3)–C antibonding character. The two important π interactions are provided by FO's 45 and 47. FO 45 is highly localized on Fe(1) and Fe(2), and best overlap with $COCH_3$ 2π or CH p_x is achieved with the orthogonal geometry. For similar reasons to the σ interaction, this π_x interaction is

(52) Kolis, J. W.; Holt, E. M.; Shriver, D. F. *J. Am. Chem. Soc.* **1983**, *105*, 7307.
(53) Whitmire, K. H.; Lagrone, C. B.; Rheingold, A. L. *Inorg Chem.* **1986**, *25*, 2472.

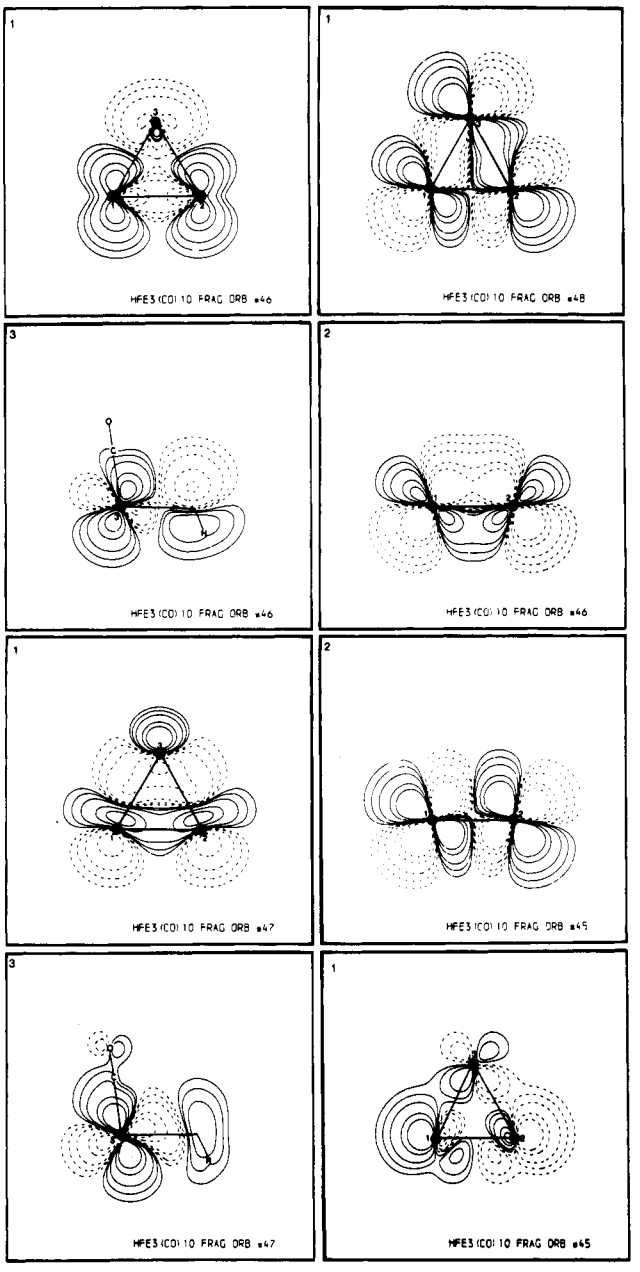

Figure 10. Contour plots of the fragment orbitals 45–48 of $Fe_3(\mu\text{-H})(CO)_{10}$: view 1, parallel to and 0.5 Å above Fe_3 plane; view 2, perpendicular to Fe_3 plane through Fe(1)–Fe(2); view 3, perpendicular to Fe_3 plane and Fe(1)–Fe(2) through Fe(3).

destabilized by movement of CR toward the centroid. A μ_2-bonding mode for the CR ligand with orthogonal geometry is thus strongly favored by these interactions. FO 48 is an in-plane orbital (bonding between Fe(1)–Fe(3) and Fe(2)–Fe(3) with the same symmetry (a″) as FO 45. It has however negligible overlap with the orbitals of the CR fragment, when the latter is in the orthogonal geometry, and is thus essentially nonbonding.

The other π-type interaction, with p_y of CH and 3π of $COCH_3$, is provided by FO 47. In this case however overlap is not optimized with the orthogonal geometry. FO 47 is distributed more evenly around the Fe_3 triangle, with slightly greater density at Fe(3), and overlap improves considerably as the CR unit moves forward Fe(3). Due to retention of the mirror symmetry of the "$Fe_3(\mu\text{-H})(CO)_{10}$" fragment in **1b**, the electronic structure of the methylidyne complex is more clearly analyzed.

The HOMO of **1b**, MO 49, is derived almost exclusively from FO 48, which is nonbonding and hence hardly perturbed in energy. MO 50 is the in-phase combination of FO 47 and p_y but, due to poor overlap, is only slightly stabilized. The antibonding combination, the virtual MO 47, is just above the LUMO in energy and is relatively isolated. The FO 45–p_x interaction is much greater, giving rise to considerable stabilization. Figure 11 shows the change in energies of MO's 49–51, the important filled frontier orbitals of **1b**, on introducing a "semi-μ_3" interaction. As the CR group is tilted, the HOMO MO 49 rises in energy. This is due to mixing in of FO 45 and p_x in an out-of-phase fashion, so that an antibonding cluster CH component is introduced. FO 48 has now increasing overlap with p_x and mixes with the in-phase combination of FO 45 and p_x (MO 51 in the orthogonal case) to result in some small stabilization. MO 50 is strongly stabilized, and the energy gain outweighs the destabilization of the HOMO. It is this stabilization that is the driving force for the "semi-μ_3" interaction, the exact extent depending on both steric and electronic factors and the nature of the alkylidyne substituent.

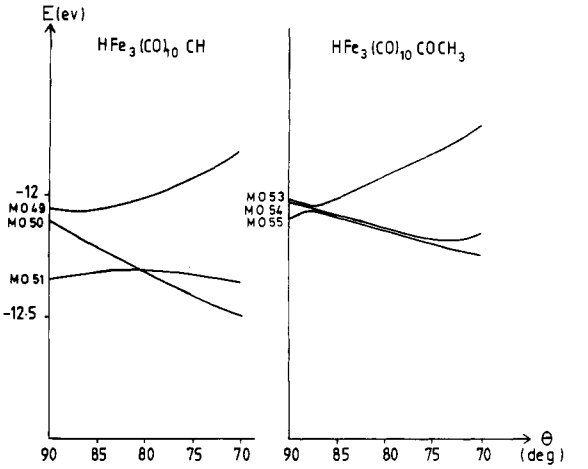

Figure 11. Correlation diagram for the frontier orbitals of $Fe_3(\mu\text{-H})(\mu\text{-CH})(CO)_{10}$.

Table VI. Overlap Populations Involving the CH Group in $Fe_3(\mu\text{-H})(\mu_3\text{-CH})(CO)_{10}$

	$\theta = 90°$	$\theta = 70°$ [a]
Fe(1)–C Fe(2)–C	0.676	0.645 (0.643)
Fe(3)–C	0.075	0.175 (0.211)
C–H	0.782	0.781 (0.790)
Fe(3)–H	−0.004	−0.038 (−0.030)
C–C_{CO}	0.048	0.107 (0.055)

[a] Figures in parentheses refer to calculations with a 10° $Fe(CO)_4$ tilt.[20]

The principle interactions in the methoxymethylidyne complex **1a** (Figure 9) are qualitatively similar. FO 47 is only slightly stabilized by interaction with 3π, due to the latter lying at higher energy relative to CH p_y and having a smaller coefficient at the carbon atom. The in-phase combination is the HOMO MO 53. Marginally below this lies MO 54, an in-phase combination of FO 45 and 2π, with considerable FO 48 character (in-phase). MO 55 is a similar orbital with an out-of-phase FO 48 admixture. The more complex derivation of these frontier orbitals for **1a** arises from the lack of mirror symmetry. The LUMO for both **1a** and **1b** is an essentially unperturbed FO 44, an in-plane σ Fe–Fe antibonding orbital very similar in character to those of complexes **3a**[36] and **4**. Figure 11 shows that for **1a** the stabilization of the π_y interaction as the $COCH_3$ ligand becomes semibridging is not great and is outweighed by the destabilization of the HOMO. A "semi-μ_3" bridge in this case is not energetically favorable,

Table VII. Experimental Data for Crystallographic Studies

	3a	4
formula	$C_{11}H_3Co_3O_{10}$	$C_{15}H_8Fe_3O_9$
M_r	471.94	499.70
space group	$P\bar{1}$ (No. 2, C_i^1)	$P2_1/n$ (No. 14, C_{2h}^5)
cryst system	triclinic	monoclinic
a/Å	8.0215 (6)	9.336 (2)
b/Å	8.3823 (4)	18.896 (2)
c/Å	12.3052 (7)	9.936 (2)
α/deg	93.011 (5)	
β/deg	102.025 (5)	99.65 (2)
γ/deg	104.890 (5)	
V/Å^3	777.12 (9)	1728.0 (6)
Z	2	4
D_{calcd}/g cm^{-3}	2.02	1.92
$F(000)$	460	992
μ(Mo Kα), cm^{-1}	32.1	25.3
T/K	298	298
scan mode	$\theta/2\theta$	$\theta/2\theta$
θ range/deg	$1.5 \leq \theta \leq 30$	$2 \leq \theta \leq 25$
cryst size/mm	0.22 × 0.32 × 0.34	0.3 × 0.3 × 0.3
cryst faces	⟨100⟩, ⟨011⟩, ⟨001⟩, ⟨011⟩	
range of transmissn coeff correctn	0.411–0.534	0.819–1.149
no. of data collected	4827	3348
no. of unique data	4525	3037
R(merge) (before abs correctn)	0.017	0.085
R(merge) (after abs correctn)	0.016	0.052
std reftctns	$\bar{3}3\bar{5}$, $\bar{4}0\bar{4}$, $\bar{5}\bar{1}3$	$\bar{3}$,10,2, $3\bar{6}\bar{4}$
observability criterion n ($I > n\sigma(I)$)	2.5	2.5
no. of data used in refinement	3528	2131
no. of refined parameters	229	244
final R	0.026	0.032
R_w	0.035	0.044
largest remaining feature in electron density diff map, e Å^{-3}	+0.44 (max), −0.53 (min)	+0.46 (max), −0.36 (min)
shift/esd in last cycle of refinement		
max	0.36	0.055
av	0.02	0.007

mainly due to the weaker interaction between FO 47 and 3π.

Table VI shows Mulliken overlap populations for **1b**, with $\theta = 90°$ and 70°. While there is only a small decrease in the Fe(1)–C and Fe(2)–C populations for $\theta = 70°$ (implying only slight loss of bonding between these centers), there is a significant rise in the Fe(3)–C population. When the $Fe(CO)_4$ group is tilted by 10°,[20] there is a further rise, suggesting improved overlap in this geometry. Interestingly the C–H and Fe(3)H overlap populations are barely affected, in line with Shapely's view[17] that the "semi-μ_3" interaction is not of the agostic-type. It may be pertinent to note that FO 47 has substantial contributions from the p_y orbitals of the CO ligand on Fe(3) cis to the μ-CH group (Figure 10). The complexes $M_3(\mu\text{-H})(\mu_3\text{-CH})(CO)_{10}$ (M = Ru,[54] Os[55]) are known to convert thermally to the tautomers $M_3(\mu\text{-H})_2(\mu_3\text{-CCO})(CO)_9$, a process involving migration of a carbonyl group from the metal to the alkylidyne carbon. In the "semi-μ_3" geometry there is a significant bonding component between the relevant carbon centers (Table VI).

There is an additional distinction between the electronic structure of **1a** and **1b**, in that **1b** possesses an isolated virtual orbital MO 47 that has substantial (ca. 50%) CH p_y character. There is no single similar orbital for **1a**, although MO's 51 (8%), 50 (16%), and 49 (8%) carry some alkylidyne character. It is suggested that the electrophilic behavior observed for $Os_3(\mu\text{-H})(\mu_3\text{-CH})(CO)_{10}$[17] is frontier orbital controlled in the manner outlined by Kostić and Fenske[37,56] for mononuclear alkylidynes. The lesser electrophilic character in the methoxymethylidyne compound is thus due to the lack of a similar virtual orbital.

Finally it should be noted that complexes of the type $M_3(\mu\text{-H})(\mu\text{-CR})(CO)_{10}$ (M = Fe, Ru, Os) may also adopt structures with symmetric μ_3-CR groups and bridging carbonyl ligands. Spectroscopic evidence suggests that $Ru_3(\mu\text{-H})(\mu_3\text{-CH})(CO)_{10}$[54] and $Fe_3(\mu\text{-H})(\mu_3\text{-CCH}_3)(CO)_{10}$[57] are of this type. Evidently the alkylidyne bonding mode depends on a fine balance of steric and electronic factors.[43] Indeed $[Fe_3(\mu_3\text{-CCH}_3)(CO)_{10}]^-$[58] and $Fe_2Ni(\mu_3\text{-COCH}_3)(\mu_3\text{-CO})(CO)_6(\eta\text{-C}_5H_5)$[11] show the presence of two isomers (presumably with μ_3- and semi-μ_3-CR groups) in solution IR spectra, indicating these differing geometries are close in energy.

Experimental Section

Instrumentation and general experimental techniques were as previously reported.[11] $Co_2(CO)_8$ was used as received from Strem and $Fe_3(\mu\text{-H})(\mu\text{-COCH}_3)(CO)_{10}$ prepared by the literature method.[11]

Reaction of $Fe_3(\mu\text{-H})(\mu\text{-COCH}_3)(CO)_{10}$ with $Co_2(CO)_8$. $Fe_3(\mu\text{-H})(\mu\text{-COCH}_3)(CO)_{10}$ (0.49 g, 1 mmol) and $Co_2(CO)_8$ (0.34 g, 1 mmol) in toluene (30 mL) were heated at 80 °C for 20 h. Removal of volatiles, followed by extraction with petroleum ether (bp 40–60 °C) afforded a dark colored solution. Chromatography on Florosil, using petroleum ether as an eluant, afforded in order of elution indigo $Co_3(\mu_3\text{-COCH}_3)(CO)_9$, purple-red unreacted $Fe_3(\mu\text{-H})(\mu\text{-COCH}_3)(CO)_{10}$, and dark brown $Co_4(CO)_{12}$. Recrystallization of the first band from petroleum ether afforded black prisms of $Co_3(\mu_3\text{-COCH}_3)(CO)_9$ (0.15 g, 48% based on Co): mass spectrum, m/e 471.7749; IR (CCl_4) ν_{CO} 2102 (w), 2050 (vs), 2036 (s), 2013 (m) 1995 (vw, br) cm^{-1}; ^{1}H NMR (−30 °C, $CDCl_3$) δ 4.03 (s, 3 H, CH_3); $^{13}C\{^1H\}$ (ambient temperature, CD_2Cl_2) δ 200.6 (s, 9 C, CO), 68.9 (s, 1 C, CH_3). Anal. Calcd for $C_{11}H_3Co_3O_{10}$: C,

(54) Holmgren, J. S.; Shapley, J. R. *Organometallics* **1984**, *3*, 1322.
(55) Shapley, J. R.; Strickland, D. S.; Strickland, D. S.; St. George, G. M.; Churchill, M. R.; Bueno, C. *Organometallics* **1983**, *2*, 185.
(56) Kostić, N. M.; Fenske, R. F. *Organometallics* **1982**, *1*, 489.
(57) Vites, J.; Fehlner, J. P. *Organometallics* **1984**, *3*, 491.
(58) Lourdichi, M.; Mathieu, R. *Nouv. J. Chim.* **1982**, *6*, 231.

27.97; H, 0.64. Found: C, 26.20; H, 0.56.

Crystal Structure Determinations. Details of data collection procedures, structure solution, and refinement are given in Table VII. Data were collected on an Enraf-Nonius CAD4F automated diffractometer, with graphite-monochromated X-radiation (λ = 0.71069 Å). Unit cell parameters were determined by refinement of the setting angles ($\theta \geq 12°$) of 25 reflections. Standards were measured every 2 h during data collection, and a linear correction was applied for complex **3a**. Lorentz, polarization, and absorption corrections were applied to both data sets, by Gaussian quatrature[59] for **3a** and by the method of Stuart and Walker[60] for **4**. Structures were solved by direct methods (MITHRIL[61]) and subsequent electron density difference syntheses. Hydrogen atoms were included in calculated positions for **4** (Cp C–H = 1.084 Å; Me C–H = 1.079 Å) and held fixed with fixed (0.05 Å^3) isotropic thermal parameters. Hydrogen atoms for **3a** were included at observed positions and thermal and positional parameters freely refined. Refinement was by full-matrix least squares, minimizing the function $\sum w(|F_o| - |F_c|)^2$ with the weighting function $w = [\sigma^2(F_o)]^{-1}$ used and judged satisfactory. $\sigma(F_o)$ was estimated from counting statistics. All non-hydrogen atoms were allowed anisotropic thermal motion. Scattering factors were taken from ref 62 with corrections applied for anomalous dispersion. All calculations were carried out on a Gould-SEL 32/27 mini computer, using the GX suite of programs.[63]

Extended Hückel Calculations. Extended Hückel calculations[64,65] were carried out by using the programs ICON8 and FMO.[66] Orbital exponents and H_{ii}'s for Fe and Co were obtained from previous work.[36] Geometries were taken from the crystal structures and idealized to C_{3v} for "$Co_3(CO)_9$" and C_s for "$Fe_3(\mu\text{-}CO)_2(CO)_6(\eta\text{-}C_5H_5)$" and "$Fe_3(\mu\text{-}H)(CO)_{10}$". Bond distances (Å) used were as follows: **3**: Co–Co = 2.478, Co–C_{alk} = 1.9, Co–C_{CO} = 1.8, C–O(carbonyl) = 1.15 Å. **4**: Fe–Fe = 2.56, Fe–C_{alk} = 1.936, Fe–C_{CO}(term) = 1.80, Fe–C_{CO}(bridge) = 1.80, 2.10, C–O(carbonyl) = 1.15 Å. **1**: Fe–Fe = 2.667, Fe–C_{alk} = 1.85, Fe–C_{CO}(term) = 1.75, C–O(carbonyl) = 1.15 Å. The same geometries were used for the alkylidyne groups throughout: CH, C–H = 1.1 Å; $COCH_3$, C–O = 1.32, O–C_{CH_3} = 1.43, C–H = 1.073 Å, and ∠C–O–C = 120°; CCH_3, C–C = 1.54 and C–H = 1.085 Å. All calculations were carried out on an ICL 2988. Orbital contour plots (at intervals of 0.05, 0.1, 0.2, 0.5, and 0.8 au^{-3}) were drawn by using the program PSI77.[67]

Registry No. **1a**, 55992-19-3; **1b**, 87698-64-4; **3a**, 41362-64-5; **4**, 101224-56-0; $Co_2(CO)_8$, 10210-68-1; $Co_3(\mu_3\text{-}CH)(CO)_9$, 15664-75-2; $Co_3(\mu_3\text{-}CCH_3)(CO)_9$, 13682-04-7; Co, 7440-48-4; Fe, 7439-89-6.

Supplementary Material Available: Tables of anisotropic thermal parameters for non-hydrogen atoms and calculated hydrogen atom positional parameters and complete listings of bond lengths and angles for **3a** and **4** (6 pages); listings of calculated and observed structure factors for **3a** and **4** (30 pages). Ordering information is given on any current masthead page.

(59) Coppens, P. *Crystallographic Computing*; Munksgaard: Copenhagen, 1970.
(60) Walker, N.; Stuart, D. *Acta Crystallogr., Sect. A: Found. Crystallogr.* **1983**, *A39*, 158.
(61) Gilmore, C. J. *J. Appl. Crystallogr.* **1984**, *17*, 42.
(62) *International Tables for X-Ray Crystallography*; Kynoch Press: Birmingham, 1974; Vol. 4.
(63) Mallinson, P. R.; Muir, K. W. *J. Appl. Crystallogr.* **1985**, *18*, 51.
(64) Hoffmann, R. *J. Chem. Phys.* **1963**, *39*, 1397.
(65) Hoffmann, R.; Lipscomb, W. N. *J. Chem. Phys.* **1962**, *36*, 2179.
(66) Howell, J.; Rossi, A.; Wallace, D.; Haraki, K.; Hoffmann, R. *QCPE* **1977**, *10*, 344.
(67) Jorgensen, W. L. "PSI77", *QCPE* **1977**, *10*, 340.

Molybdenum–Molybdenum and Phosphorus–Phosphorus or Sulfur–Sulfur Bond Cleavage Reactions of Organic Substrates with Compounds Containing a Metal–Metal Triple Bond

Howard Alper,*[†1a] Frederick W. B. Einstein,*[1b] Frederick W. Hartstock,[1a] and Richard H. Jones[1b]

Departments of Chemistry, University of Ottawa, Ottawa, Ontario, Canada K1N 9B4, and Simon Fraser University, Burnaby, British Columbia, Canada V5A 1S6

Received July 29, 1986

Reaction of the metal–metal triple-bonded complexes $(RC_5H_4)_2Mo_2(CO)_4$ (R = H, CH_3) with tetraalkyldiphosphine disulfides $[R_2'P(S)P(S)R_2']$ affords the mononuclear complexes $(R_2'PS)Mo(CO)_2(C_5H_5\text{-}\eta^5)$ in which the $R_2'PS$ unit acts as a three-electron ligand. A single-crystal X-ray analysis of one such complex (R = R′ = CH_3) revealed that the phosphorus–sulfur bond distance [2.003 (2) Å] was in between that of a typical PS single and double bond. Crystals of this complex are orthorhombic with a = 6.643 (2) Å, b = 13.643 (5) Å, c = 13.902 (3) Å, Z = 4, and space group $P2_12_12_1$. The structure was refined by full-matrix least-squares techniques to R_F = 0.026 and R_{wF} = 0.030 for 1355 reflections with $I > 3\sigma(I)$. Dithiocarbamate complexes were obtained when thiuram disulfides were used as the substrates. The structure of one such complex, $(\eta^5\text{-}C_5H_5)Mo(CO)_2[S_2CN(CH(CH_3)_2)_2]$, was confirmed by X-ray analysis. Crystals of the dithiocarbamate are triclinic with a = 7.800 (1) Å, b = 10.186 (3) Å, c = 10.250 (3) Å, α = 79.10 (3)°, β = 85.26 (2), γ = 83.63 (2)°, Z = 2, and space group $P\bar{1}$. The structure was refined by full-matrix least-squares techniques to R_F = 0.038 and R_{wF} = 0.051 for 2356 reflections with $I > 3\sigma(I)$.

A wide variety of interesting reactions have been observed by using cyclopentadienylmolybdenum dicarbonyl dimer **1**, R = H, a compound containing a metal–metal triple bond, and organic substrates.[2,3] Use of organosulfur and organophosphorus compounds as reactants usually results in addition to the organometallic complex. For example, cyclic sulfides such as tetrahydrothiopyran undergo nucleophilic addition to **1**, R = H, affording **2** where the heterocyclic functions as a bridging ligand.[4] Com-

[†] John Simon Guggenheim Fellow, 1985–1986. Killam Research Fellow, 1986–1988.

(1) (a) University of Ottawa. (b) Simon Fraser University.
(2) Cotton, F. A.; Walton, R. A. *Multiple Bonds Between Metal Atoms*; Wiley; New York, 1982.
(3) Curtis, M. D.; Messerle, L.; Fontinos, N. A. In *Reactivity of Metal-Metal* Bonds; ACS Symposium Series No. 155; American Chemical Society: Washington, DC, 1981; pp 221–257 and references cited therein.

0276-7333/87/2306-0829$01.50/0